

Supplementary Information:

**Adsorption Behavior of Ionic and Nonionic Surfactants on
Polymer Surfaces**

Giulia Magi Meconi¹, Nicholas Ballard¹, José M. Asua¹, and Ronen Zangi^{2,3}

¹POLYMAT & Departamento de Química Aplicada, Facultad de Ciencias Químicas, University of the Basque Country UPV/EHU, Avenida de Tolosa 72, 20018, Donostia–San Sebastián, Spain

²POLYMAT & Departamento de Química Orgánica I, University of the Basque Country UPV/EHU, Avenida de Tolosa 72, 20018, Donostia–San Sebastián, Spain

³IKERBASQUE, Basque Foundation for Science, María Díaz de Haro 3, 48013 Bilbao, Spain

October 19, 2016

Table S1: Details of the simulation setups for the three surfactants studied. For each surfactant we considered four concentrations reported as two-dimensional densities, ρ_{2D} . The molecule, 16-mer PS, composing the surface is defined in Fig. S1. The average length of the simulation box along each axis is also shown.

	# Surfactants	ρ_{2D} [mg/m ²]	# 16-mer PS	# Waters	$\langle X \rangle / \langle Y \rangle$ [nm]	$\langle Z \rangle$ [nm]
SDS	1 / 12 / 24 / 48	0.0365 – 1.71	20	2853 – 2973	3.62 – 3.67	10.71 – 12.11
7PEO4PE	1 / 8 / 12 / 24	0.0551 – 1.34	20	3491 – 6560	3.58 – 3.64	12.10 – 20.07
10PEO6PE	1 / 8 / 12 / 24	0.0545 – 1.38	22	3949 – 11417	4.25 – 4.37	9.37 – 22.05

A Model for Poly(styrene)

A PS chain is modeled as a 16-mer unit. Because the stereochemistry of each unit is randomly generated during polymerization, we chose to model each chain with alternating C_α chiral centers (R followed by S). The bonded and non-bonded parameters of PS were taken from the OPLS-AA model of ethylbenzene^{1,2}. However, in order to allow the connectivity between the subunits and simultaneously maintain zero charge for each of these subunits, we made the following changes. The partial charge of C_β of the first residue was changed from -0.180 to -0.120, that of C_γ of the last residue was changed from -0.115 to -0.055, and both changes were applied to the repeating residues. The resulting model is shown in Fig. S1 and the non-bonded interactions are specified in Table S2. Using this model, we obtained a value of 1.02 kg/m³ for the density of amorphous PS which is close to its experimental value³ of 1.04–1.06 kg/m³. Furthermore, the calculated values of the radius of gyration, 9.8 Å, and the weight-normalized end-to-end distance squared, 0.42 Å²·mol/g, are also in a very good agreement with their experimentally determined values of 10.0 Å and 0.43 Å²·mol/g, respectively, as well as with other models for PS^{4–6}.

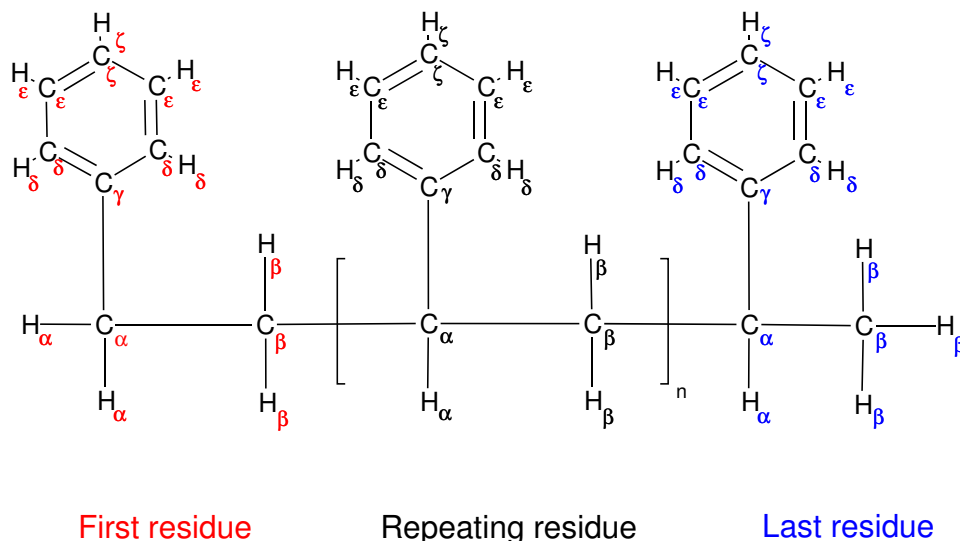


Figure S1: The model for poly(styrene) based on the OPLS-AA force-field. The partial charge and LJ parameters describing each atom is detailed in Table S2. Note that the C_α of the repeating and last residues are chiral, nevertheless, the parameters for the R and S configurations are the same.

Table S2: Partial charges and LJ parameters for the poly(styrene) model. The values refer to all residue types (first, repeating, and last) unless otherwise indicated.

	q [e]	σ [nm]	ϵ [kJ/mol]
C_α	-0.005	0.350	0.276
C_β	-0.120	0.350	0.276
$C_{\beta, \text{last}}$	-0.180	0.350	0.276
C_γ	-0.055	0.355	0.293
$C_{\gamma, \text{first}}$	-0.115	0.355	0.293
H_α, H_β	+0.060	0.250	0.126
$C_\delta, C_\epsilon, C_\zeta$	-0.115	0.355	0.293
$H_\delta, H_\epsilon, H_\zeta$	+0.115	0.242	0.126

A Model for Sodium Dodecyl Sulfate

Bonded and nonbonded parameters for SDS were adopted from the model of Shelley et al.^{7,8}. However, because this model integrates the hydrogens of the methyl and methylene groups into the carbons to which they are connected, we performed quantum calculations, following the RESP (Restrained Electrostatic Potential) charge fitting procedure⁹, to determine the partial charges in these groups. Bonded interactions that were missing for the all-atom description were taken from the corresponding interactions of the OPLS-AA force-field. The resulting model is displayed in Fig. S2 and the non-bonded parameters in Table S3. The LJ parameters of the sodium counterion, $\sigma=0.333$ nm and $\epsilon=0.0116$ kJ/mol, were taken from the OPLS-AA force-field.

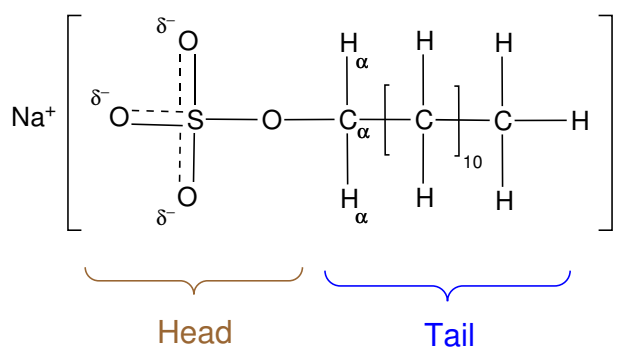


Figure S2: The model for SDS surfactant. The partial charge and LJ parameters describing each atom is detailed in Table S3.

Table S3: Partial charges and LJ parameters for the SDS model. The atoms are divided according to their association to the head or tail groups.

	q [e]	σ [nm]	ϵ [kJ/mol]
Head			
S	+1.284	0.355	1.046
O	-0.654	0.315	0.837
O _{ester}	-0.459	0.300	0.711
Tail			
C _{α}	+0.077	0.350	0.276
H _{α}	+0.030	0.242	0.063
C	-0.120	0.350	0.276
C _{last}	-0.180	0.350	0.276
H	+0.060	0.250	0.126

A Model for poly(ethylene oxide)-poly(ethylene)

For the PEO-PE surfactant, we considered molecules with two different lengths. The shorter surfactant, labeled as 7PEO4PE, is $\text{HO} - (\text{CH}_2\text{CH}_2\text{O})_7 - (\text{CH}_2)_7 - \text{CH}_3$. The longer surfactant, labeled as 10PEO6PE, is $\text{HO} - (\text{CH}_2\text{CH}_2\text{O})_{10} - (\text{CH}_2)_{11} - \text{CH}_3$ to which Disponil AFX1080 was compared experimentally. Results from a self-consistent field theory predicts that the head size of the surfactant influences the adsorption significantly¹⁰. Parameters for the PE and PEO segments of the surfactant were taken from the OPLS-AA force-field¹¹. For the latter, the values were derived from dimethyl ether group. The model for this surfactant is given in Fig. S3 and Table S4.

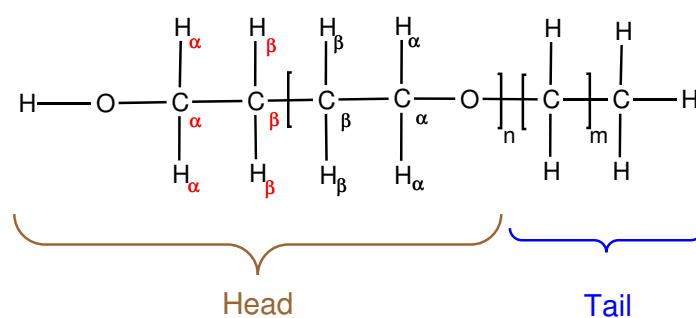


Figure S3: The model for PEO-PE surfactant. The partial charge and LJ parameters describing each atom is detailed in Table S4.

Table S4: Partial charges and LJ parameters for the PEO-PE surfactant model. The atoms are divided according to their association to the head or tail groups.

	q [e]	σ [nm]	ϵ [kJ/mol]
Head			
$C_{\alpha,\beta}$	+0.140	0.350	0.276
$C_{\alpha,first}$	-0.015	0.350	0.276
$H_{\alpha,\beta}$	+0.030	0.250	0.126
$H_{\alpha,first}$	+0.040	0.250	0.126
O	-0.400	0.290	0.586
O_{first}	-0.683	0.312	0.711
H_{first}	+0.418	0.000	0.000
Tail			
C	-0.120	0.350	0.276
C_{last}	-0.180	0.350	0.276
H	+0.060	0.250	0.126

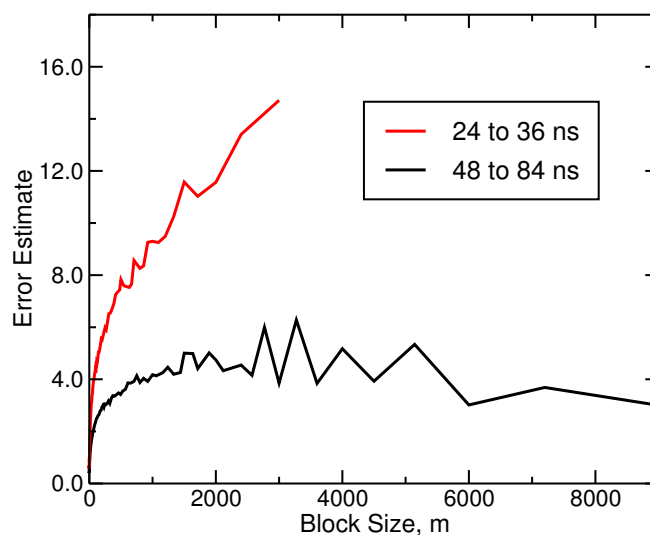


Figure S4: Analysis of the convergence of the constrained force along different segments of the trajectory for 10PEO6PE with 24 surfactants at $d_c=0.103$ nm. This point is in the vicinity of the equilibrium adsorbed state and convergence required longer simulation. In order to obtain an estimate for the error we used the block averaging method. The trajectory is divided into n number of blocks of equal size m and averages are calculated for each block. The error for the total average is calculated from the variance between the averages of the n blocks. The curves show this error estimate as a function of the block size m . The plot for the earlier and shorter segment of the trajectory (24–36 ns) continues to increase as the block size increases (or the number of blocks decreases) whereas the last and longer segment of the trajectory (48–84 ns) exhibits a plateau (and even a slight decrease due to sufficient number of blocks which are large enough) which signifies convergence.

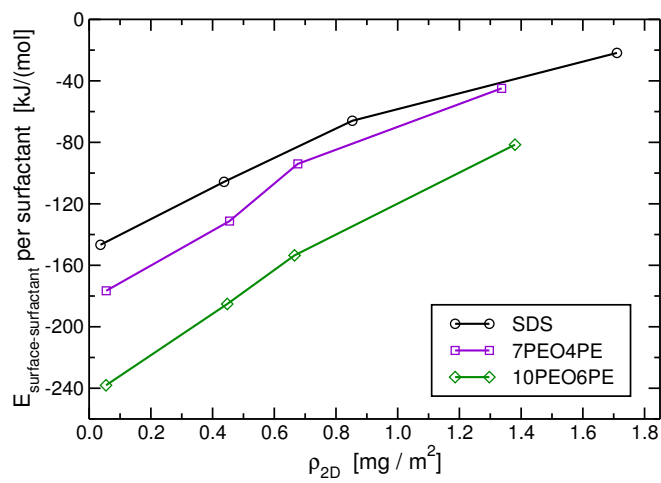


Figure S5: The surface-surfactant energy per surfactant as a function of the 2D-density.

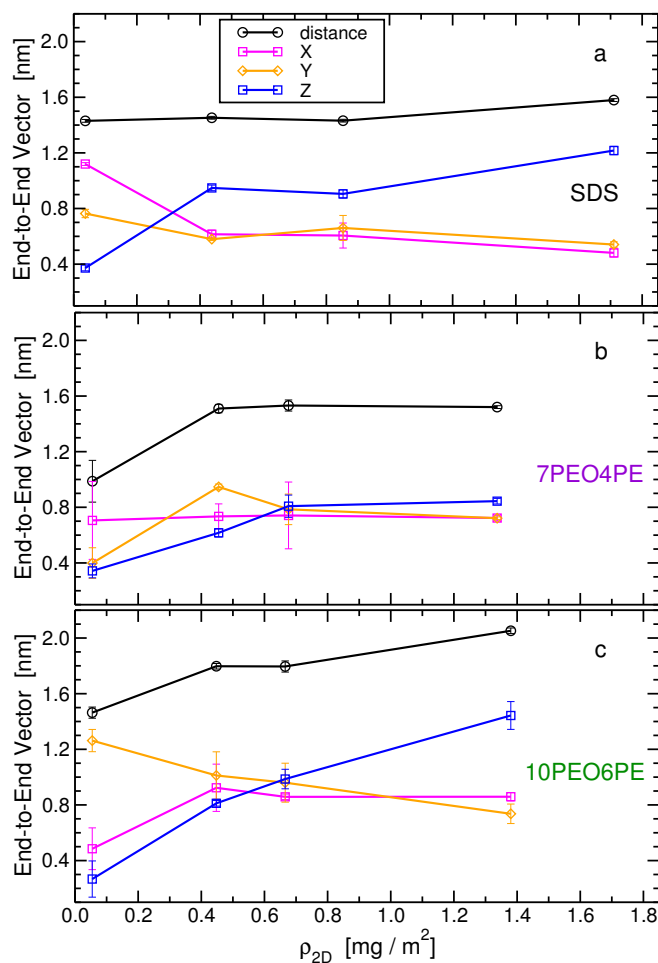


Figure S6: The end-to-end vector of the surfactant (between the heavy atoms at both ends) as a function of the 2D-density. The plots show the scalar distance as well as the projections parallel (x and y) and normal (z) to the interface plane. This analysis is performed for the equilibrium points (adsorbed state) of the pulling processes shown in Fig. 5 averaged over the last 36 ns of the trajectories. Error bars are displayed, however, in some cases their size is comparable to the size of the symbols.

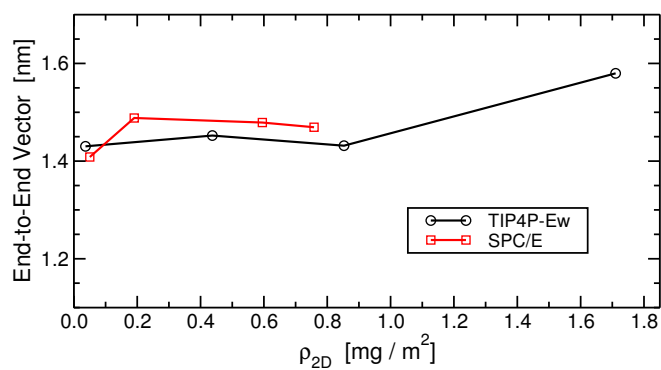


Figure S7: Comparison of the end-to-end distance (between the heavy atoms at both ends) of the SDS surfactants from simulations in which the water molecules were described by the TIP4P-Ew and SPC/E water models.

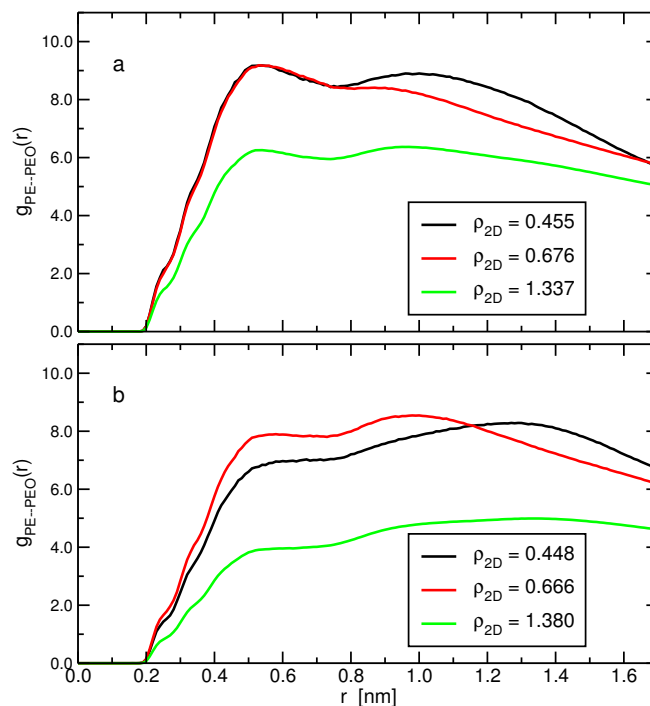


Figure S8: The radial distribution functions between the tail atoms (the PE segment) and head atoms (the PEO segment excluding the connecting $-\text{CH}_2\text{CH}_2\text{O}-$ group) of different surfactants for different 2D-densities for the (a) 7PEO4PE and (b) 10PEO6PE systems. The analyzes are computed for the equilibrium points of the pulling processes shown in Fig. 5 averaged over the last 36 ns of the trajectories.

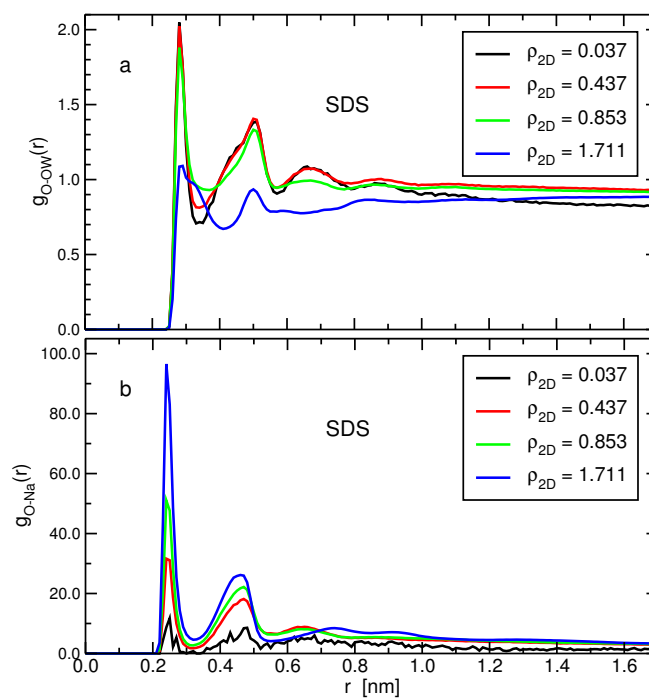


Figure S9: The radial distribution functions between the oxygen atoms of SDS and (a) the oxygen atoms of water, (b) the sodium cations, at different two-dimensional densities. The analyzes are computed for the equilibrium points (adsorbed state) of the pulling processes shown in Fig. 5 averaged over the last 36 ns of the trajectories.

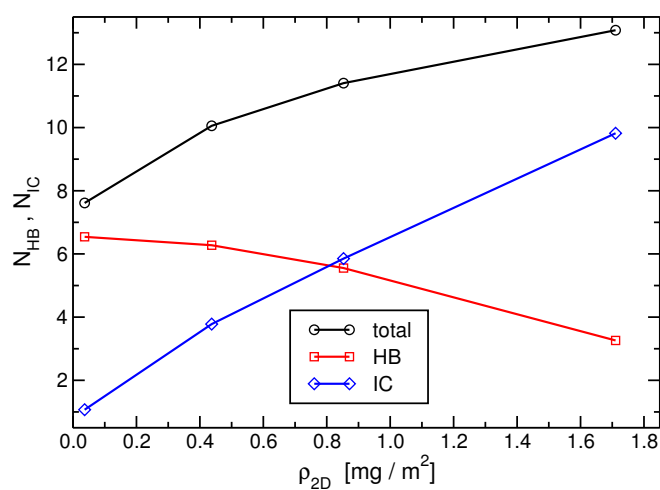


Figure S10: The number of hydrogen bonds and the number of ion contacts, per surfactant, between SDS molecules and the solvent as a function of the 2D-density. The analysis is performed in the adsorbed state.

The Effect of the Chain Stiffness

In order to investigate the effect of the stiffness of the nonionic surfactants on the structure of the adsorbed layer at the interface with the PS surface, we performed additional simulations for the long and short surfactants in which their dihedral angles were characterized by a much stiffer potentials ($V_d = k_\phi [1 + \cos(n\phi)]$ with $k_\phi=10$ kJ/mol, $\phi=180^\circ$, and $n=3$). For each system we considered 12 surfactants in exactly the same conditions as with the unperturbed systems except for the number of water molecules which were 4300 and 10500 for the 7PEO4PE and 10PEO6PE surfactants, respectively. The resulting 2D-densities were $\rho_{2D}=0.681$ and 0.702 mg/m² which are to be compared with the $\rho_{2D}=0.666$ and 0.676 mg/m² of the unperturbed OPLS-AA force-field for the short and long surfactants, respectively. The simulations were run in the adsorbed state for 100 ns and data were collected for 36 ns.

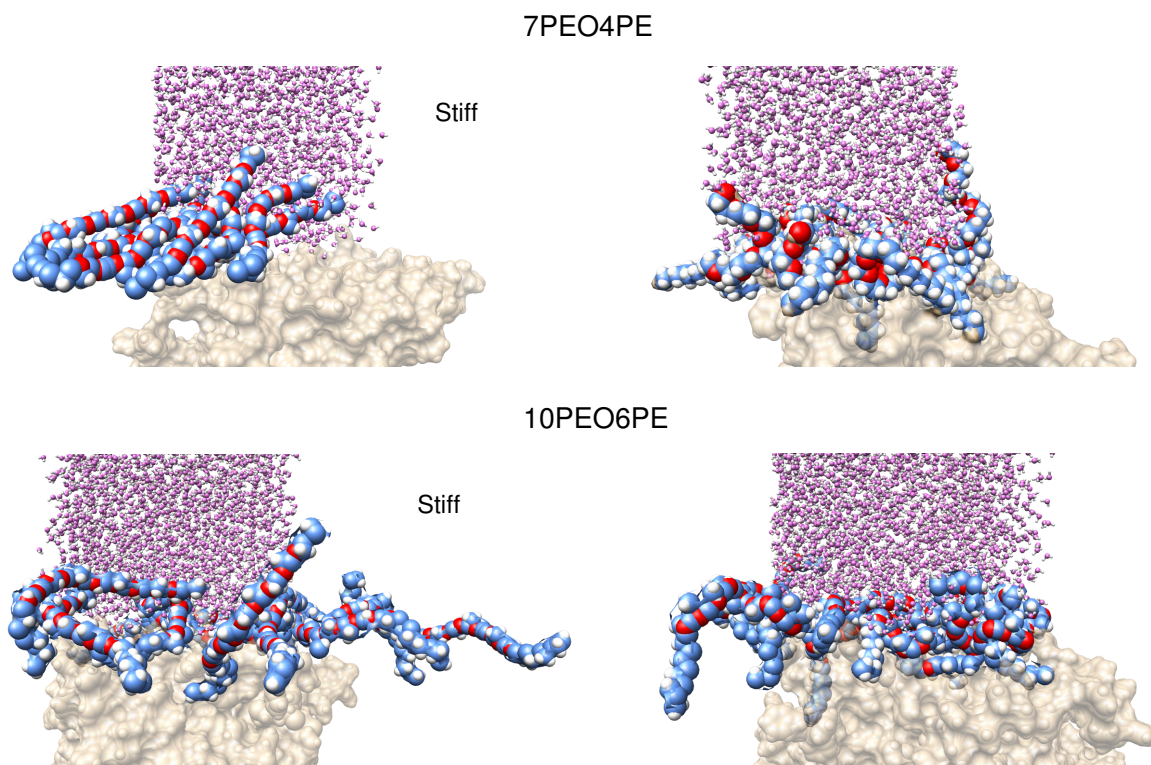


Figure S11: Snapshots from the simulations with the stiff nonionic surfactants described above (left panel) compared with those with unperturbed OPLSAA force field (right panel).

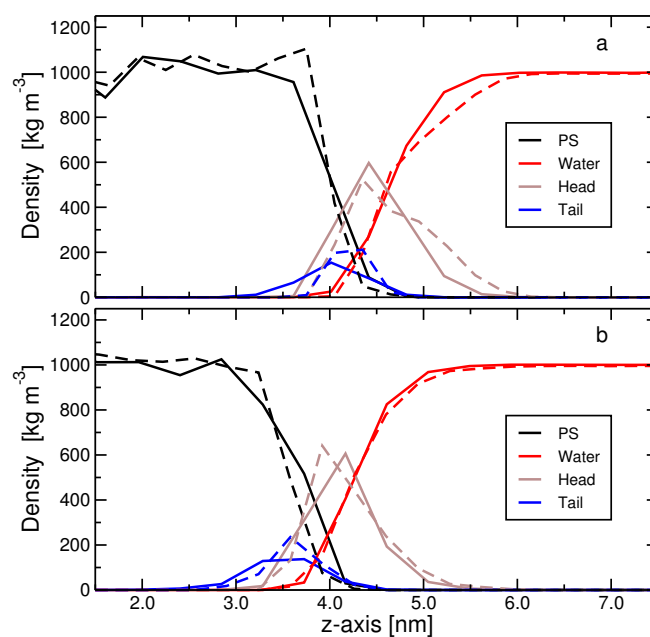


Figure S12: The density profiles of the system with the stiff (dashed lines) nonionic surfactants compared with those with the unperturbed OPLSAA force-field (solid lines) for the (a) 7PEO4PE and (b) 10PEO6PE systems. The profiles were superimposed on top of each other in such a way to maximize the overlap of the curves for the water phase.

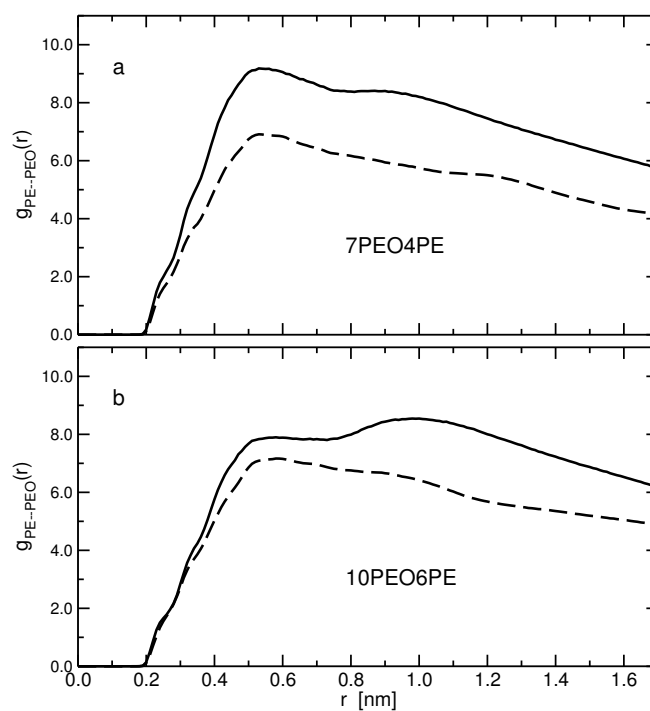


Figure S13: The radial distribution functions between the tail atoms (the PE segment) and head atoms (the PEO segment excluding the connecting $-\text{CH}_2\text{CH}_2\text{O}-$ group) of different surfactants for the system with stiff (dashed lines) nonionic surfactants compared with those with unperturbed OPLSAA force-field (solid lines) for the (a) 7PEO4PE and (b) 10PEO6PE systems.

Table S5: The end-to-end distance, as well as its three components, of the surfactants with the stiff dihedral angles compared to those with the unperturbed dihedrals. In the last row we provide the number of hydrogen bonds, per surfactant, between the surfactants (head groups) and the water molecules.

	7PEO4PE		10PEO6PE	
End-to-End	stiff	unperturbed	stiff	unperturbed
distance	2.03	1.53	2.33	1.80
X	1.10	0.74	1.43	0.86
Y	1.23	0.79	1.34	0.96
Z	0.99	0.81	1.02	0.99
HB	5.0	6.1	6.2	7.9

References

- [1] Jorgensen, W. L.; Severance, D. L. Aromatic-Aromatic Interactions: Free Energy Profiles for the Benzene Dimer in Water, Chloroform and Liquid Benzene, *J. Am. Chem. Soc.* **1990**, *112*, 4768–4774.
- [2] Price, M. L. P.; Ostrovsky, D.; Jorgensen, W. L. Gas-Phase and Liquid-State Properties of Esters, Nitriles, and Nitro Compounds with the OPLS-AA Force Field, *J. Comp. Chem.* **2001**, *22*, 1340–1352.
- [3] Brandrup, J.; Immergut, E. H.; Grulke, E. A. *Polymer Handbook*; Wiley: New York, fourth ed., 2003.
- [4] Fetters, L. J.; Lohse, D. J.; Richter, D.; Witten, T. A.; Zirkel, A. Connection between Polymer Molecular Weight, Density, Chain Dimensions, and Melt Viscoelastic Properties, *Macromolecules* **1994**, *27*, 4639–4647.
- [5] Harmandaris, V. A.; Adhikari, N. P.; van der Vegt, N. F. A.; Kremer, K. Hierarchical Modeling of Polystyrene: From Atomistic to Coarse-Grained Simulations, *Macromolecules* **2006**, *39*, 6708–6719.
- [6] Spyriouni, T.; Tzoumanekas, C.; Theodorou, D.; Müller-Plathe, F.; Milano, G. Coarse-Grained and Reverse-Mapped United-Atom Simulations of Long-Chain Atactic Polystyrene Melts: Structure, Thermodynamic Properties, Chain Conformation, and Entanglements, *Macromolecules* **2007**, *40*, 3876–3885.
- [7] Shelley, J.; Watanabe, K.; Klein, M. L. Simulation of a sodium dodecylsulfate micelle in aqueous solution, *Int. J. Quant. Chem.* **1990**, *38*, 103–117.
- [8] Schweighofer, K. J.; Essmann, U.; Berkowitz, M. Simulation of Sodium Dodecyl Sulfate at the Water-Vapor and Water-Carbon Tetrachloride Interfaces at Low Surface Coverage, *J. Phys. Chem. B* **1997**, *101*, 3793–3799.
- [9] Bayly, C. I.; Cieplak, P.; Cornell, W.; Kollman, P. A. A well-behaved electrostatic potential based method using charge restraints for deriving atomic charges: the RESP model, *J. Phys. Chem.* **1993**, *97*, 10269–10280.

- [10] Jódar-Reyes, A. B.; Ortega-Vinuesa, J. L.; Martín-Rodríguez, A.; Leermakers, F. A. M. Self-Consistent Field Model of Inhomogeneous Adsorption of Nonionic Surfactants onto Polystyrene Latex, *Langmuir* **2003**, *19*, 878–887.
- [11] Jorgensen, W. L.; Maxwell, D. S.; Tirado-Rives, J. Development and Testing of the OPLS All-Atom Force Field on Conformational Energetics and Properties of Organic Liquids, *J. Am. Chem. Soc.* **1996**, *118*, 11225–11236.